Jamming Resistance Capabilities of Spectrally Phase Encoded OCDMA Communication Systems With Optimum and Suboptimum (Nonlinear Two-Photon-Absorption) Receiver Structures

Mohammad J. Emadi and Jawad A. Salehi, *Senior Member, IEEE*

***Abstract*—In this paper, we study three types of jammers, namely, pulse-jammer, partial-band jammer, and follower-jammer, in a typical fiber-optic-based spectrally phase-encoded optical code division multiple-access (SPE-OCDMA) system. We analyze, mathematically, the effects of the aforementioned jammers on the performance of an SPE-OCDMA system for two scenarios, namely, ideal noiseless channel with an ideal optimum receiver and an ultrahigh-speed nonlinear receiver based on two-photon-absorption (TPA) in a noisy channel. Also, for each of the above cases, two types of modulation, namely, ON–OFF keying (OOK) and two-code keying (2CK) are investigated and their system performances are compared. It is shown that under certain conditions, the system performance can be dramatically degraded due to the jamming signals; also, systems using 2CK modulation show a better resistance and performance when compared to systems using OOK modulation.**

***Index Terms*—Jammer, on–off keying modulation, optical code division multiple access, resistance capabilities, spectrally phase encoded, two-code keying modulation, two-photon-absorption.**

I. Introduction

ENHANCED security is often mentioned as one of the key benefits of spectrally phase-encoded optical code division multiple-access (SPE-OCDMA) systems [1]. However, the margin and the degree of various security enhancement have not been considered deeply in the literature. One of the criteria in determining the degree of security of a system is to assess its resistance capabilities against various jammers and attacks. In SPE-OCDMA system, coding is applied to the phase of frequency spectrum of the ultrashort light pulses. Thus, at the receiver front end the desired user's data signal shape is a noise-like Gaussian with low intensity and can be simply separated from multiple-access interference (MAI) by simple match filtering (decoding). In this scheme, the properly decoded signals convert in to their original pulse shapes, and improperly decoded signals remain as noise-like Gaussian with low intensity, equivalent to temporarily broadened signals [1]–[3].

Thus, as a consequence of this noise-like Gaussian behavior, the security of the system is enhanced, and it is considered as one of the advantages of the SPE-OCDMA systems. At first glance, this conclusion, i.e., security enhancement, seems reasonable. In general, the adversary tries to impose his control over the communication of the information and its objectives can be categorized as follows: 1) intercepting the information furtively and 2) transmitting jamming signals to prevent successful communication for the target user [4]. The first objective is introduced and analyzed in [5]–[8]. It is demonstrated that the SPE-OCDMA systems with OOK modulation do not have security at all. The interceptor can easily break the system security nonwith simple energy detector without requiring knowledge about the spreading code. This vulnerability of the system against eavesdropper can be somehow evaded by sending equal energy for transmitting data bits of "1" and "0" (by using different encoders); this modulation is called 2CK. So, using this type of modulation and utilizing balanced detection not only the system security improves but also the optimum threshold due to the symmetry of transmission is zero, and it is also independent of the number of users and the amount of power used by the users [5]–[9].

The technology advancement in optical communication makes it possible that even in fiber environment, the adversary can tap in or by other means jam the target users. Although various applications of SPE-OCDMA have found their place in research and industry [10], performance of such schemes against various jammers have not been investigated in literature previously.

In this paper, we cover jamming issues and we introduce three types of jamming signals and evaluate their effects on a typical SPE-OCDMA system. In order to investigate jamming resistance and capabilities of SPE-OCDMA system, we have considered two scenarios. In the first scenario, we assume optimum and ideal receiver structure and neglect all source of noise except multiple access. In general, the bandwidth of photodetectors is less than the bandwidth of transmitted optical signals; hence, as a result, the performance of SPE-OCDMA systems decreases [11]. Among a few solutions to improve the system performance is to utilize ultrahigh-speed nonlinear TPA receiver structure. Thus, in second scenario, the resistance capabilities of SPE-OCDMA system with TPA receiver structure is ana-

Manuscript received March 18, 2009; revised June 20, 2009. First published July 07, 2009; current version published September 17, 2009. This work was supported in part by Iran National Science Foundation (INSF).

The authors are with the Optical Networks Research Laboratory (ONRL), Electrical Engineering Department, Sharif University of Technology, Tehran, Iran (e-mail: emadi@ee.sharif.ir; jasalehi@sharif.edu).

Color versions of one or more of the figures in this paper are available online at http://ieeexplore.ieee.org.

Digital Object Identifier 10.1109/JLT.2009.2027030

0733-8724/$26.00 © 2009 IEEE

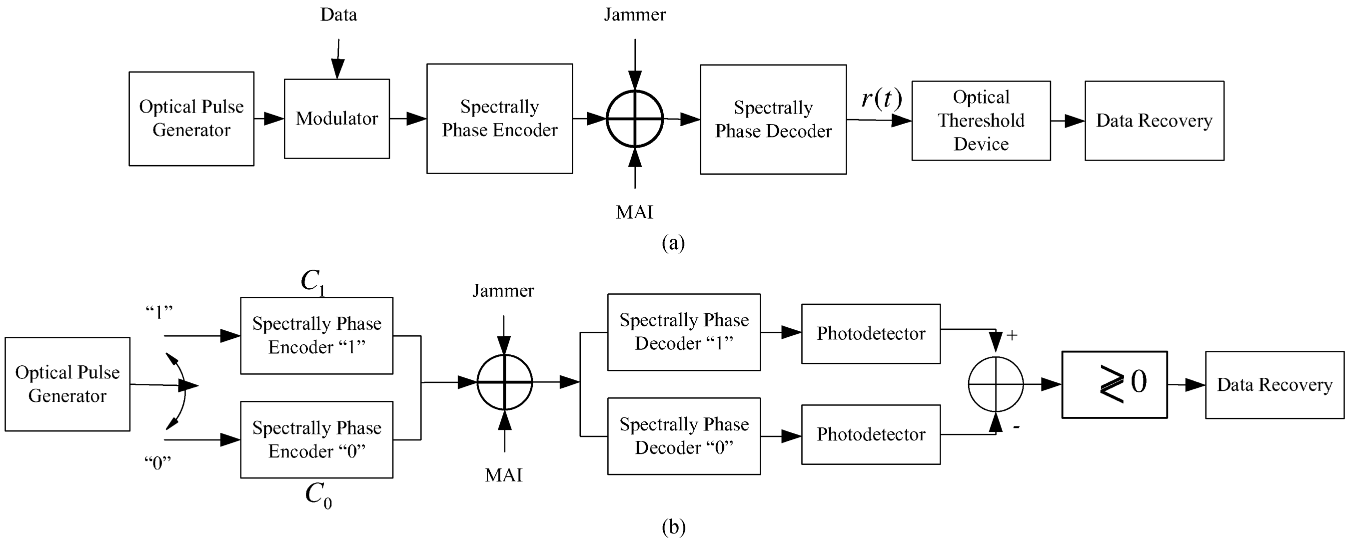

Fig. 1. Typical block diagram of $U \times U$, SPE-OCDMA system: (a) OOK modulation; (b) $2\mathrm{CK}$ modulation.

lyzed. Also, for each scenario, we have investigated resistance of the system for two types of modulations, i.e., OOK and 2CK modulations.

The rest of the paper is organized as follows. In Section II, we introduce the system under the consideration with optimum detection scheme. In Section III, three types of jammers are introduced, and the performance of the system with two types of modulation scheme in various jamming environments are evaluated. In Section IV, the noisy system with nonlinear TPA receiver structure is introduced, and the system performance in different jamming environments for both modulations' schemes is evaluated. In Section V, numerical evaluation of the system performance for different structures is discussed. Finally, we conclude the paper in Section VI.

II. Multiple-Access System's Description With Optimum Detection Scheme in Jamming Environment

In our system's description, we assume that all users have the same bit rate and transmit the same pulse format; in addition, each user uses random encoding as their spectral signature sequence. In this system, we ignore both the thermal and quantum noises, but the system performance is sensitive to MAI and jamming signals. Fig. 1(a) shows a typical $U \times U$, OOK SPE-OCDMA system, where U is the number of users. The kth user's initial ultrashort light pulses are characterized by a baseband Fourier spectrum, $A_k(\omega)$ given by [1]

$$A_k(\omega)=\begin{cases} \sqrt{\frac{P_0}{W}}, & -\frac{W}{2} \leq \omega \leq \frac{W}{2} \\ 0, & \text{elsewhere} \end{cases}, \quad k=1,2,\ldots,U \tag{1}$$

where P_0 is the peak power of the ultrashort light pulse and W is the total bandwidth of the band-limited mode-locked laser (MLL) pulse. To encode the coherent pulse, the initial spectrum of the pulse is multiplied by a spectral-phase code, which consists of N_0 frequency chips, each of bandwidth $\Omega = W/N_0$, where the phase of each frequency chips can be either -1 or $+1$ with equal probability. Post encoding, the duration of encoded pulses stretch to $T \cong N_0 T_c$, where T_c is the duration of the original incident pulse. Note that from (1) $T_c = 2\pi/W$. In general, the time duration of each user's data source, T_b, can be larger than T, so $K \triangleq T_b/T$, and its effect on the performance is considered in [1], [11], [12]. It is assumed that the ith user is the target user. As Fig. 1(a) shows, the received signal of the ith user, $r(t)$ can be written as

$$r(t) = E_{ii}(t) + E_{Ji}\left(t - t'_{Ji}\right) + \sum_{k\neq i}^{U-1} E_{ki}\left(t - t'_{ki}\right) \tag{2}$$

where $E_{ii}(t)$ is the properly decoded signal of the ith user, $E_{Ji}(t - t'_{Ji})$ is the improperly decoded signal of the jammer, and $E_{ki}(t - t'_{ki})$ is the improperly decoded signal of the kth user at the output of the ith target user. The intensity of the received signal is given by

$$I(t) = r(t) \times r^*(t) \tag{3}$$

where "$*$" stand for complex conjugate operation.

However, in SPE-OCDMA system using $2\mathrm{CK}$ modulation, each transceiver has two encoders and two decoders, one pair for data bit "1" and another for data bit "0." At the receiver end, the output of decoder "0" is subtracted from the output of decoder "1," and the result is compared with zero [13]. Fig. 1(b) shows a simplified structure for a 2CK SPE-OCDMA system.

III. Performance Analysis of SPE-OCDMA System in Various Jamming Environments

In the following sections, building upon previously introduced SPE-OCDMA system with optimum detection scheme, as shown in Figs. 1, we analyze the performance of the system in different jamming environments for two types of modulations, namely, OOK and 2CK modulations.

A. Performance Analysis of an Ideal Noiseless SPE-OCDMA System in Various Jamming Environments With OOK Modulation

In the following, three types of jamming signals are modeled and discussed, and the systems performance are evaluated analytically for various jamming environments.

1) Pulse-Jammer: A pulse-jammer (PJ) sends similar pulses as the pulses of the MLL used by the users of the network but with higher power compared to the pulses of SPE-OCDMA users. This jammer sends its pulses over a fraction of time with spectral amplitude of $\sqrt{(J/\rho)/W}$, where W is the bandwidth of the MLL pulse, and ρ (duty factor) is the probability that the jammer is ON and transmits its pulses [see Fig. 2(a)]. In this figure, we have eight jamming pulses in 40 data bits; hence, $8/40 = 0.2$, i.e., $\rho \cong 0.2$. When the jammer is ON, the transmitted power is J/ρ, but the average power transmitted by the jammer is a constant "J." Therefore, the jamming pulses are characterized by a baseband Fourier spectrum $A_{\mathrm{PJ}}(\omega)$, and it is given as [see Fig. 2(b)]

$$A_{\mathrm{PJ}}(\omega) = \begin{cases} \sqrt{\frac{J/\rho}{W}}, & -\frac{W}{2} \le \omega \le \frac{W}{2} \\ 0, & \text{elsewhere} \end{cases}. \tag{4}$$

For our pulse-jamming scenario, it is assumed that the duration of the transmitted jamming pulses is more than the duration of one information bit (T_b); so, the transmitted bits of the target user encounters the jamming pulses over the channel with probability ρ and does not encounter the jamming pulses with probability $(1-\rho)$ [14]. Hence, the probability of error (P_e) can be expressed as

$$\begin{aligned} P_e &= P_r(\text{PJ is on}) \cdot P_r(\text{error}|\text{PJ is on}) \\ &\quad + P_r(\text{PJ is off}) \cdot P_r(\text{error}|\text{PJ is off}) \\ &= \rho \cdot P_r(\text{error}|\text{PJ is on}) + (1-\rho) \\ &\quad \cdot P_r(\text{error}|\text{PJ is off}). \end{aligned} \tag{5}$$

In the following, the effect of PJ on the performance of the system (P_e) with OOK modulation is investigated. Furthermore, an attempt will be made to find ρ_{opt} to maximize P_e. In OOK modulation, users send a pulse for bit "1" and do not send any form of pulse for bit "0." At the target user's spectrally phase decoder output, the signal of the jammer is spectrally phase encoded; so, it obtains the same characteristics such as MAI signals. Therefore, we can write the probability density function (pdf) of the received intensity (I) as [1]

$$\begin{aligned} P\left(I|d_i^{(k)}, l, \mathrm{PJ}\right) &= \frac{1}{((P_0/N_0)l + (J/\rho N_0))} \\ &\quad \cdot \exp\left(\frac{-\left(I + d_i^{(k)} P_0\right)}{(P_0/N_0)l + (J/\rho N_0)}\right) \\ &\quad \cdot I_0\left(\frac{\sqrt{I P_0 d_i^{(k)}}}{(P_0/N_0)l + (J/\rho N_0)}\right) . U(I) \end{aligned} \tag{6}$$

where l is the number of MAI, $I_0(x)$ is the modified Bessel function of the first kind and zeroth order, $U(I)$ is the unit step function, and $d_i^{(k)} \in \{0, 1\}$ is kth transmitted data of ith user. Then, the conditional probability of error can be evaluated as

$$\begin{aligned} P_{e|l,\mathrm{PJ}} &= P_r(\text{error}|l, \mathrm{PJ}) = \frac{1}{2}(P_{\mathrm{FA}|l,\mathrm{PJ}} + P_{\mathrm{MD}|l,\mathrm{PJ}}) \\ &= \frac{1}{2}\left[\int_{\mathrm{Th}}^{\infty} P\left(I|d_i^{(k)} = 0, l, \mathrm{PJ}\right) dI \right. \\ &\quad \left. + \int_{-\infty}^{\mathrm{Th}} P\left(I|d_i^{(k)} = 1, l, \mathrm{PJ}\right) dI \right] \end{aligned} \tag{7}$$

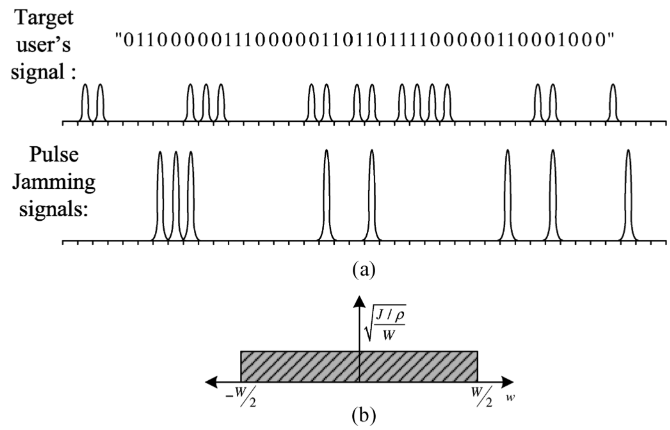

Fig. 2. Representation of transmitting pulse jamming signals: (a) time domain; (b) baseband Fourier spectrum of PJ's signals.

where $P_{e|l,\mathrm{PJ}}$ is the probability of error given PJ and l interfering users that transmit their ON data bits on the same time slot as the target user's data time slot. "Th" is the threshold of the receiver, $P_{\mathrm{FA}|l,\mathrm{PJ}}$ is the probability that MAI plus jamming signal cross "Th," i.e., false alarm, and $P_{\mathrm{MD}|l,\mathrm{PJ}}$ is the probability that the combination of transmitting "1" in the presence of the interference and jamming signal do not cross "Th," i.e., miss detection. It is assumed that the target user's threshold is set at optimum threshold to minimize P_e. Thus, $P_{\mathrm{FA}|l,\mathrm{PJ}}$ can be evaluated as [1]

$$P_{\mathrm{FA}|l,\mathrm{PJ}} = \exp\left(-\frac{N_0(\mathrm{Th_{opt}}/P_0)}{l + (\mathrm{JSR}/\rho)}\right) \tag{8}$$

where $\mathrm{JSR} = J/P_0$ is the jammer to signal ratio and also $P_{\mathrm{MD}|l,\mathrm{PJ}}$ can be evaluated as [1]

$$P_{\mathrm{MD}|l,\mathrm{PJ}} = 1 - Q\left(\sqrt{\frac{2N_0}{l + \mathrm{JSR}/\rho}}, \sqrt{\frac{2N_0(\mathrm{Th_{opt}}/P_0)}{l + \mathrm{JSR}/\rho}}\right) \tag{9}$$

where $Q(x, y)$ is the Marcum's Q-function. Substituting (8) and (9) in (7) and averaging over number of interferences and PJ being ON or OFF, we can write the unconditional error probability P_e as follow:

$$P_e = \sum_{l=0}^{U-1} \left(\rho . P_{e|l,\mathrm{PJ}} + (1-\rho) . P_{e|l,\mathrm{PJ}=0}\right) . p_{\mathrm{OOK}}(l) \tag{10}$$

when $\mathrm{PJ} = 0$ is equal to $\mathrm{JSR} = 0$, i.e., the PJ is OFF, and $p_{\mathrm{OOK}}(l)$ is the probability of the presence of l interfering users that transmit ON data on the target user's data pulse. $p_{\mathrm{OOK}}(l)$ can be written as

$$p_{\mathrm{OOK}}(l) = \binom{U-1}{l} \left(\frac{1}{2K}\right)^l \left(1 - \frac{1}{2K}\right)^{U-1-l} \tag{11}$$

where $(U-1)$ is the number of interfering users and K is equal to the ratio of the bit period (T_b) to the encoded pulse duration $(N_0 T_c)$, i.e., $K = \lfloor T_b / N_0 T_c \rfloor$.

2) Partial-Band Jammer: For a partial-band jammer (PBJ), the jammer sends ultrashort light pulses that are characterized by a baseband Fourier spectrum, $A_{\mathrm{PBJ}}(\omega)$, given as (see Fig. 3)

$$A_{\mathrm{PBJ}}(\omega) = \begin{cases} \sqrt{\frac{J}{W_J}}, & -\frac{W_J}{2} \le \omega \le \frac{W_J}{2} \\ 0, & \text{elsewhere} \end{cases} \tag{12}$$

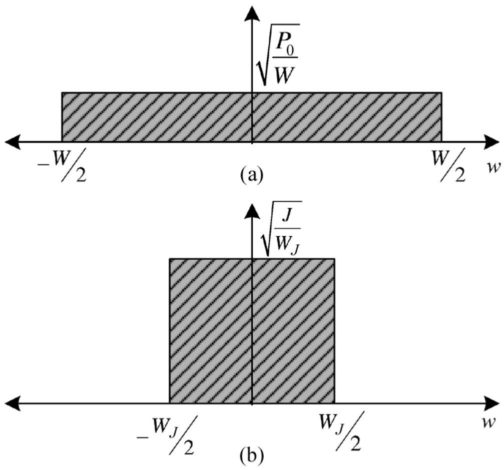

Fig. 3. Baseband Fourier spectrum: (a) target user's initial ultrashort light pulse spectrum; (b) PBJ's signal spectrum.

where J is the peak power of the jamming pulse and W_J is the total bandwidth of the band-limited source of the jammer. W_J can be written as

$$W_J \triangleq (2M+1)\Omega = M_0\Omega \quad : \quad 1 \le M_0 \le N_0. \tag{13}$$

Equation (13) implies that the spectrum of PBJ pulses only see M_0 bins of the random phase code instead of N_0 bins. Therefore, we can say that the transmitted signal of PBJ covers a fraction, i.e., M_0/N_0, of the spectrum of the transmitted pulse of the user. The signal of the PBJ when passing through the decoder of the target user sees a code with length M_0 and reduces to a noise-like signal with power J/M_0.

Per our prior discussion, the behavior of PBJ in the presence of l interfering users at the receiver output of the target user has an intensity probability distribution equal to

$$P\left(I|d_i^{(k)}, l, \mathrm{PBJ}\right) = \frac{1}{((P_0/N_0)l + (J/M_0))} \cdot \exp\left(-\frac{I + d_i^{(k)}P_0}{(P_0/N_0)l + (J/M_0)}\right) \cdot I_0\left(\frac{\sqrt{IP_0 d_i^{(k)}}}{(P_0/N_0)l + (J/M_0)}\right).U(I). \tag{14}$$

If we define $\mathrm{JSR} \triangleq J/P_0$, and $\rho_{\mathrm{PBJ}} \triangleq M_0/N_0$, similar to the PJ, we can write the conditional probability of error $(P_{e|l})$ as (6). Similar to (6), we can compute $P_{\mathrm{FA}|l}$ and $P_{\mathrm{MD}|l}$ analytically, and they can be expressed as

$$P_{\mathrm{FA}|l} = \exp\left(-\frac{N_0\left(\mathrm{Th_{opt}}/P_0\right)}{l + (\mathrm{JSR}/\rho_{\mathrm{PBJ}})}\right) \tag{15}$$

and

$$P_{\mathrm{MD}|l} = 1 - Q\left(\sqrt{\frac{2N_0}{l + \mathrm{JSR}/\rho_{\mathrm{PBJ}}}}, \sqrt{\frac{2N_0(\mathrm{Th_{opt}}/P_0)}{l + \mathrm{JSR}/\rho_{\mathrm{PBJ}}}}\right). \tag{16}$$

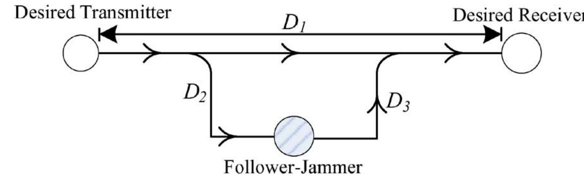

Fig. 4. Simplified structure of FJ.

Finally, we write the probability of error as

$$P_e = \sum_{l=0}^{U-1} P_{e|l} \cdot p_{\mathrm{OOK}}(l). \tag{17}$$

3) Follower-Jammer: For a follower-jammer (FJ), we first intercept the channel; then, after processing the intercepted channel signal, we send it back on the channel continually. Fig. 4 shows a simplified structure of the target user's transceiver in an FJ scenario. Let $((D_2+D_3)/(c/n))+T_{pr} \le (D_1/(c/n))+T_b$, where T_{pr} is the required time for the FJ to process the intercepted signal, T_b is the duration of a bit, c is the velocity of the light, n is the index of fiber, and D_i: $i = 1, 2, 3$ are relative distances. It can be concluded that the jamming signal in the current bit duration is processed from the previous bit interval and since signals in different bit durations are independent, then the jamming signal is independent from the MAI and the target's signal of the current bit duration, i.e., signal d_i. When FJ intercepts the channel, in addition to the target user's signal, i.e., signal d_J, it generates l_J interferences due to other users. For the worst-case scenario, we let the loss of the jammer path be L dB and the jamming signal is synchronous with the transmitted signal of the target user. Thus, the received signal at the target receiver end can be written as

$$r(t) = (\sqrt{G}d_i + \sqrt{L}d_J)E_{ii}(t) + \sqrt{G}\sum_{j\neq i}^{l} E_{ij}(t) + \sqrt{L}\sum_{j\neq i}^{l_J} E_{ij}(t) \tag{18}$$

where G is the total gain through user's path. We investigate four possible scenarios and compute the probability of error for all cases. The pdf of the received intensity, I, at the output of the receiver for OOK modulation $(d_J, d_i \in \{0,1\})$ is

$$P_{d_J,d_i}(I) = P(I|d_J, d_i, l_J, l) = \frac{1}{\sigma^2} \cdot \exp\left(-\frac{I + (d_i + \sqrt{L}d_J)^2 P_0}{\sigma^2}\right) .I_0\left(\frac{\sqrt{I(d_i + \sqrt{L}d_J)^2 P_0}}{\sigma^2}\right).U(I) \tag{19}$$

where $\sigma^2 = (P_0/N_0)(l + l_J L)$. When the target user transmits d_i, we can compute conditional probability of errors as follow:

$$P_{e|d_J,d_i=0} = P_r(I > Th_{\mathrm{opt}}|d_J, 0, l_J, l), \quad d_J = 0, 1 \tag{20}$$

and

$$P_{e|d_J,d_i=1} = P_r(I \le Th_{\mathrm{opt}}|d_J, 1, l_J, l,), \quad d_J = 0, 1 \tag{21}$$

so, $P_{e|0,0}$ can be evaluated as

$$P_{e|0,0} = \exp\left(-\frac{\mathrm{Th_{opt}}/P_0}{l+l_J L} N_0\right) \tag{22}$$

similar to [1], $P_{e|d_J,d_i}$, $\forall (d_J, d_i) \in \{(0,1),(1,0),(1,1)\}$ can be indicated as

$$P_{e|1,0} = Q\left(\sqrt{\frac{2LN_0}{l+l_J L}}, \sqrt{\frac{2N_0(\mathrm{Th_{opt}}/P_0)}{l+l_J L}}\right) \tag{23}$$

$$P_{e|0,1} = 1-Q\left(\sqrt{\frac{2N_0}{l+l_J L}}, \sqrt{\frac{2N_0(\mathrm{Th_{opt}}/P_0)}{l+l_J L}}\right) \tag{24}$$

$$P_{e|1,1} = 1-Q\left(\sqrt{\frac{2(1+\sqrt{L})^2 N_0}{l+l_J L}}, \sqrt{\frac{2N_0(\mathrm{Th_{opt}}/P_0)}{l+l_J L}}\right) \tag{25}$$

where $Q(.,.)$ is Marcum's Q-function. Finally averaging over l and l_J, the probability of error can be obtained as

$$P_e = \frac{1}{4}\sum_{l=0}^{U-1}\sum_{l_J=0}^{U-1}\left\{\left(P_{e|0,0}+P_{e|0,1}+P_{e|1,0}+P_{e|1,1}\right) \times p_{\mathrm{OOK}}(l)\, p_{\mathrm{OOK}}(l_J)\right\} \tag{26}$$

where $p_{\mathrm{OOK}}(l_J) = p_{\mathrm{OOK}}(l)|_{l=l_J}$.

B. $2CK$ Modulation in Jamming Environment With Optimum Detection

Per our previous discussion, at the receiver end for 2CK modulation, the encoded signal passes through the decoder and a pair of balanced photodiodes receiver. The balanced photodiodes receiver provides subtraction of random variable I_{C_0} from I_{C_1}. Random variables I_{C_0} and I_{C_1} correspond to the output intensity of decoders C_0 and C_1, respectively [9]. Hence, the final receiver output can be expressed as $\Delta I = I_{C_1} - I_{C_0}$. ΔI is a random variable and its corresponding pdf in various jamming environments is evaluated in the following sections.

1) Pulse-Jammer: First, we assume that the target user transmits bit "1." Consequently, at the output of decoder C_1, there are l interfering signals due to MAI, one noise-like signal due to the jammer, and a pulse due to the properly decoded of the target signal. So, $P_{I_{C_1|1}}(I)$ is evaluated as

$$\begin{aligned} P_{I_{C_1|1}}(I) &= P(I|d_i=1,l,\mathrm{PJ}) \\ &= \frac{1}{((P_0/N_0)l+(J/\rho N_0))}\exp\left(-\frac{I+P_0}{(P_0/N_0)l+(J/\rho N_0)}\right) \\ &\quad\times I_0\left(\frac{2\sqrt{IP_0}}{(P_0/N_0)l+(J/\rho N_0)}\right). \end{aligned} \tag{27}$$

However, at the output of decoder C_0 interfering and noise-like signals due to MAI and the PJ are similar to the output of decoder C_1, but the transmitted signal due to the target user is improperly decoded, as a result we have another noise-like signal. So, $P_{I_{C_0|1}}(I)$ can be written as

$$\begin{aligned} P_{I_{C_0|1}}(I) &= P(I|d_i=1,l,\mathrm{PJ}) \\ &= \frac{1}{((P_0/N_0)(l+1)+(J/\rho N_0))} \\ &\quad\times \exp\left(-\frac{I}{(P_0/N_0)(l+1)+(J/\rho N_0)}\right)U(I). \end{aligned} \tag{28}$$

Since $I_{C_1|1}$ and $I_{C_0|1}$ are independent random variables, we may compute $P_{\Delta I|1}(I)$ as the convolution of $I_{C_1|1}$ and $I_{C_0|1}$ pdf, so we get (29)-(30), shown at the bottom of this page.

Now we assume that the target transmitter sends bit "0," since there is symmetry in the system, it can be shown that $P_{\Delta I|0}(I) = P_{\Delta I|1}(-I)$. Therefore, the conditional probability of error can be evaluated as

$$\begin{aligned} P_{e|l,\mathrm{PJ}} &= \frac{1}{2}\left[\int_0^{+\infty} P_{\Delta I|0}(I)dI + \int_{-\infty}^{0} P_{\Delta I|1}(I)dI\right] \\ &= \int_{-\infty}^{0} P_{\Delta I|1}(I)dI \end{aligned} \tag{31}$$

$$P_{\Delta I|1}(I) = P_{I_{C_1|1}}(I) * P_{I_{C_0|1}}(-I) \tag{29}$$

$$\begin{aligned} P_{\Delta I|1}(I) =& \frac{1}{((P_0/N_0)(l+1)+(J/\rho N_0)).((P_0/N_0)l+(J/\rho N_0))}\int_{-\infty}^{+\infty} I_0\left(\frac{2\sqrt{I'P_0}}{(P_0/N_0)l+(J/\rho N_0)}\right) \\ &\cdot\exp\left(-\frac{I'+P_0}{(P_0/N_0)l+(J/\rho N_0)}\right)\cdot\exp\left(-\frac{I-I'}{(P_0/N_0)(l+1)+(J/\rho N_0)}\right)\cdot U(I').U(I'-I).dI' \\ =& \frac{1}{((P_0/N_0)(l+1)+(J/\rho N_0)).((P_0/N_0)l+(J/\rho N_0))}\cdot\exp\left(-\frac{P_0}{(P_0/N_0)l+(J/\rho N_0)}\right) \\ &\cdot\exp\left(-\frac{I}{(P_0/N_0)(l+1)+(J/\rho N_0)}\right)\int_{max(0,I)}^{+\infty} I_0\left(\frac{2\sqrt{I'P_0}}{(P_0/N_0)l+(J/\rho N_0)}\right) \\ &\cdot\exp\left(-\frac{P_0/N_0(2l+1)+\frac{2J}{\rho N_0}}{((P_0/N_0)(l+1)+(J/\rho N_0))\,((P_0/N_0)l+(J/\rho N_0))}I'\right)\,dI'. \end{aligned} \tag{30}$$

substituting (30) in (31) and considering the integral boundaries, $P_{e|l,\mathrm{PJ}}$ can be evaluated as

$$P_{e|l,\mathrm{PJ}}=\frac{(l+1)+(\mathrm{JSR}/\rho)}{(2l+1)+(2\mathrm{JSR}/\rho)}\exp\left(-\frac{N_0}{(2l+1)+(2\mathrm{JSR}/\rho)}\right). \tag{32}$$

Averaging over PJ, i.e., being ON or OFF, and the number of multiuser interferences P_e can be written as

$$P_e=\sum_{l=0}^{U-1}\left\{\rho P_{e|l,\mathrm{PJ}}+(1-\rho)P_{e|l,\mathrm{PJ}=0}\right\}.p_{2\mathrm{CK}}(l) \tag{33}$$

where $P_{e|l,\mathrm{PJ}=0}$ can be computed from (32) by setting $\mathrm{JSR}=0$. Furthermore, $p_{2\mathrm{CK}}(l)$ can be written as

$$p_{2\mathrm{CK}}(l)=\binom{U-1}{l}\left(\frac{1}{K}\right)^{l}\left(1-\frac{1}{K}\right)^{(U-1-l)}. \tag{34}$$

2) Partial-Band Jammer: By defining $\rho_{\mathrm{PBJ}}=M_0/N_0$, then the expressions for the probability of error will be the same as the PJ, only it is necessary to replace ρ by ρ_{PBJ}. So, the conditional probability of error can be written as

$$P_{e|l}=\frac{(l+1)\rho_{\mathrm{PBJ}}+\mathrm{JSR}}{(2l+1)\rho_{\mathrm{PBJ}}+2\mathrm{JSR}}\exp\left(-\frac{N_0\rho_{\mathrm{PBJ}}}{(2l+1)\rho_{\mathrm{PBJ}}+2\mathrm{JSR}}\right). \tag{35}$$

Finally, the probability of error can be written as

$$P_e=\sum_{l=0}^{U-1}P_{e|l}.p_{2\mathrm{CK}}(l). \tag{36}$$

3) Follower-Jammer: In the presence of an FJ, it is sufficient to compute the pdf of the output of decoder C_0 and C_1 for each case. Therefore, properly or improperly decoded received signals at the output of decoder C_k, $k\in\{0,1\}$, have intensity pdf as

$$\begin{aligned}P_{I_{C_k|d_J,d_i}}(I)&=P(I|d_J,d_i,l_J,l)\\&=\frac{1}{\sigma^2_{I_{C_k|d_J,d_i}}}\exp\left(-\frac{I+m_{C_k|d_J,d_i}}{\sigma^2_{I_{C_k|d_J,d_i}}}\right)\\&\quad\times I_0\left(\frac{\sqrt{I.m_{C_k|d_J,d_i}}}{\sigma^2_{I_{C_k|d_J,d_i}}}\right)U(I)\end{aligned} \tag{37}$$

where $d_J,d_i\in\{0,1\}$. If "-" stands for "not," i.e., $\overline{0}=1,\overline{1}=0$, for the decoder C_0, we have

$$m_{C_0|d_J,d_i}=(\overline{d_i}+\overline{d_J}\sqrt{L})^2P_0 \tag{38}$$

$$\sigma^2_{I_{C_0|d_J,d_i}}=\frac{P_0}{N_0}\left(l+d_i+(l_J+d_J)L\right) \tag{39}$$

and for the decoder C_1, we can write

$$m_{C_1|d_J,d_i}=(d_i+d_J\sqrt{L})^2P_0 \tag{40}$$

$$\sigma^2_{I_{C_1|d_J,d_i}}=\frac{P_0}{N_0}\left(l+\overline{d_i}+(l_J+\overline{d_J})L\right). \tag{41}$$

When $(d_J,d_i)=(0,0)$ and if we denote $I_{00}=I_{C_1|00}-I_{C_0|00}$, the conditional probability of error can be evaluated as

$$\begin{aligned}P_{e|00}&=P_r(I_{00}>0)\\&=\frac{\sigma^2_{I_{C_1|00}}}{\sigma^2_{I_{C_0|00}}+\sigma^2_{I_{C_1|00}}}\exp\left(-\frac{(1+\sqrt{L})^2P_0}{\sigma^2_{I_{C_0|00}}+\sigma^2_{I_{C_1|00}}}\right).\end{aligned} \tag{42}$$

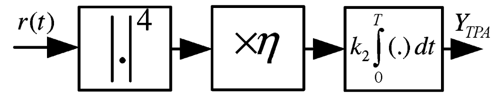

Fig. 5. Mathematical representation of an ideal TPA receiver structure.

Since there is symmetry in the system, we have $P_{e|00}=P_{e|11}$.

On the other hand when $(d_J,d_i)=(0,1)$, the output intensities of decoders C_0 and C_1 have Rician distribution, and the pdf of $I_{01}=I_{C_1|01}-I_{C_0|01}$ cannot be evaluated so easily. So, in this case, we resort to Saddle-point approximation method to compute the error probability of the system. The characteristic function of random variable $I_{C_k|01}$, can be written as

$$\Phi_{I_{C_k|01}}(s)=\frac{\exp\left((m_{C_k|01}.s)/(1-\sigma^2_{I_{C_k|01}}.s)\right)}{1-\sigma^2_{I_{C_k|01}}.s},\quad k=1,0. \tag{43}$$

Since random variables $I_{C_0|01}$ and $I_{C_1|01}$ are statistically independent, the characteristic function of I_{01} can be evaluated as

$$\Phi_{I_01}(s)=\Phi_{I_{C_1|01}}(s)\times\Phi_{I_{C_0|01}}(-s). \tag{44}$$

Using Saddle-point approximation, an excellent approximation on the probability of error ($P_{e|01}=P_r(I_{01}<0)$ can be obtained. Averaging over the number of interfering signals that are present in the jamming signals and the network, the system probability of error can be computed as follows:

$$P_e=\frac{1}{2}\sum_{l=0}^{U-1}\sum_{l_J=0}^{U-1}(P_{e|00}+P_{e|01}).p_{2\mathrm{CK}}(l).p_{2\mathrm{CK}}(l_J). \tag{45}$$

IV. Noisy System With Nonlinear TPA Receiver Structure

Optical communication is well suited for transmitting ultrahigh data rate, but the main bottleneck of such a system is switching from high-speed optical domain to low-speed electrical domain. To overcome this bottleneck, a nonlinear detection such as TPA process has been introduced [11], [15], [16]. It is shown that the rate of photoelectrons dN/dt, which is generated by TPA receiver is proportional to the square of the intensity of the light pulse in a period of T, i.e.

$$\frac{dN}{dt}=\frac{\alpha}{hf}I(t)+\frac{\gamma}{2hf}I^2(t) \tag{46}$$

where h is the Plank's constant, f is the central frequency of the received light, α is the single photon absorption coefficient, and γ is the TPA coefficient. For an ideal TPA receiver $\alpha=0$, and the number of produced photoelectrons at the output of an ideal TPA receiver end can be written as [15]

$$Y_{\mathrm{TPA}}=k_2\int_0^T I^2(t)dt \tag{47}$$

where k_2 is a constant related to the frequency and physical parameters of a TPA receiver. Fig. 5 shows an ideal TPA receiver transfer function. The mean and variance of the random variable Y_{TPA} is described in the Appendix. A typical representation of an SPE-OCDMA using TPA-receiver is depicted in Fig. 6.

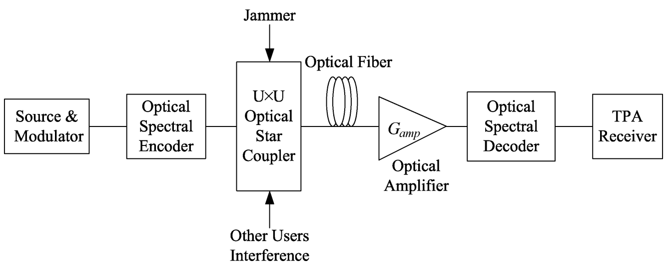

Fig. 6. Schematic of spectral-phase-encoded CDMA using optical amplifier and TPA receiver structure.

Also, concept of using OOK and 2CK modulations is similar to the noiseless with optimum detection scheme system.

A. Performance Analysis of a Noisy Channel With TPA Receiver and OOK Modulation in Various Jamming Environments

In this section, we assume OOK modulation and evaluate the system performance using Gaussian approximation. Therefore, it is only necessary to compute the mean and the variance of the random variable Y_{TPA}. Using Gaussian approximation, the optimum threshold can be computed as [17]

$$\mathrm{Th}_{\mathrm{opt}} = \frac{m_0\sigma_1 + m_1\sigma_0}{\sigma_1 + \sigma_0} \tag{48}$$

where m_0 and m_1 are the mean and σ_0^2 and σ_1^2 are the variance of the random variable Y_{TPA}, for transmitting "0" and "1," respectively. Therefore, the error probability can be computed as

$$P_e = Q\left(\frac{m_1 - m_0}{\sigma_0 + \sigma_1}\right) \tag{49}$$

where $Q(.)$ is the Q-function. In the following sections, we analyze the system performance in various jamming environments.

1) Pulse-Jammer: We have assumed that the average transmitted photons of a PJ is m_J; therefore, the noises due to optical amplification, l amplified interfering users, and PJ's signals can be added to form noise-like Gaussian variable with a power spectral density equal to N_S, which can be expressed as

$$N_s = N_T + \frac{lmG}{N_0} + \frac{m_J G}{\rho N_0} \tag{50}$$

where N_T is power spectral density of optical amplifier noise, m is the average transmitted photons of each user, and G is total gain between transmitter and receiver. Substituting (50) in (A.1)–(A.6), the mean and variance can be evaluated. Therefore, using Gaussian approximation, the error probability can be expressed as (10).

2) Partial-Band Jammer: If we assume that the number of frequency bins in the spectrum of the PBJ transmitted signal is M_0, then N_s can be rewritten as, $N_s = N_T + (lmG/N_0) + (m_J G/M_0)$. By computing the mean and the variance of random variable, Y_{TPA}, the error probability can be computed as (17).

3) Follower-Jammer: We have assumed that the transmitted signal of the FJ can be written as

$$r_J(t) = \sqrt{L} d_J E_{ii}(t') + \sqrt{L}\sum_{j\neq i}^{l_J} E_{ij}(t') \tag{51}$$

where L is the total loss through the FJ path, d_J is the emulated bits that exists in FJ transmitted signals, and l_J is the number of active users when the jammer has intercepted the channel. Therefore, the received signal at the target receiver end can be written as

$$r(t) = (\sqrt{G} d_i + \sqrt{L} d_J) E_{ii}(t) + \sqrt{G}\sum_{j\neq i}^{l} E_{ij}(t) + \sqrt{L}\sum_{j\neq i}^{l_J} E_{ij}(t) + Q(t) \tag{52}$$

where G is the total gain between the transmitter and receiver, d_i is the transmitted bit of the target user, l is the number of active user, and $Q(t)$ is the noise of the signal after passing through the star coupler and optical amplifier with power spectral density N_T of $Q(t)$ equal to [12]

$$N_T = n_{\mathrm{sp}}(G_{\mathrm{amp}} - 1)L_2 \tag{53}$$

where n_{sp} is spontaneous emission factor, G_{amp} is gain of the optical amplifier, and L_2 is total loss after the star coupler. Since the interference signals that are presented in the FJ transmitted signal, i.e., $\sqrt{L}\sum_{j\neq i}^{l_J} E_{ij}(t^)$, are independent of the interference signals that are presented in the received signal, i.e., $\sqrt{G}\sum_{j\neq i}^{l} E_{ij}(t)$, we can evaluate the average received photons, and the power spectral density of the received signal as

$$\overline{m} = m(\sqrt{G} d_i + \sqrt{L} d_J)^2 \tag{54}$$

$$N_s = N_T + \frac{m(lG + l_J L)}{N_0}. \tag{55}$$

By substituting $\overline{m}$ and N_s in (A.1) the mean and variance of Y_{TPA}, i.e., m_{d_J,d_i} and $\sigma^2_{d_J,d_i}$, can be evaluated then $Y_{\mathrm{TPA}|d_J,d_i} \sim N(m_{d_J,d_i}, \sigma^2_{d_J,d_i})$. Since $d_i, d_J \in \{0,1\}$, $Y_{\mathrm{TPA}|d_J,d_i}$ has four different states, then the conditional error probability can be evaluated as

$$P_{e|l_J,l} = \frac{1}{4}\left\{P_r(Y_{\mathrm{TPA}|00} > Th_{\mathrm{opt}}) + P_r(Y_{\mathrm{TPA}|01} < Th_{\mathrm{opt}}) + P_r(Y_{\mathrm{TPA}|10} > Th_{\mathrm{opt}}) + P_r(Y_{\mathrm{TPA}|11} < Th_{\mathrm{opt}})\right\} \tag{56}$$

computing the mean and the variance of each state, then the probabilities can be evaluated as

$$P_r(Y_{\mathrm{TPA}|d_J,0} > Th_{\mathrm{opt}}) = Q\left(\frac{\mathrm{Th}_{\mathrm{opt}} - m_{d_J,0}}{\sigma_{d_J,0}}\right) \quad \forall d_J = 0,1 \tag{57}$$

$$P_r(Y_{\mathrm{TPA}|d_J,1} < Th_{\mathrm{opt}}) = 1 - Q\left(\frac{\mathrm{Th}_{\mathrm{opt}} - m_{d_J,1}}{\sigma_{d_J,1}}\right) \quad \forall d_J = 0,1 \tag{58}$$

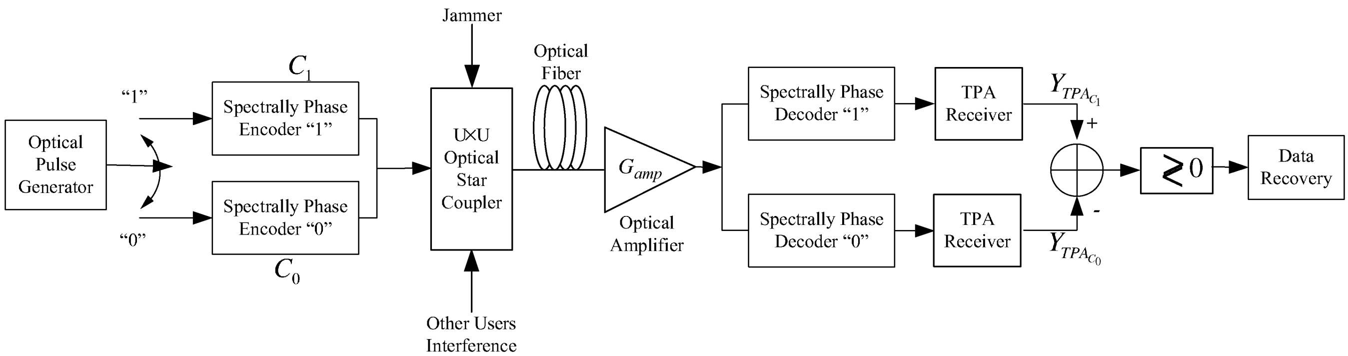

Fig. 7. Typical block diagram of $U \times U$, 2CK SPE-OCDMA system using TPA receiver structure.

therefore, the error probability can be evaluated as

$$P_e = \sum_{l=0}^{U-1} \sum_{l_J=0}^{U-1} P_{e|l_J,l} \cdot p_{\rm OOK}(l) \cdot p_{\rm OOK}(l_J). \tag{59}$$

B. $2CK$ Modulation With TPA Receiver Structure

As we discussed before, in a typical 2CK modulation structure each user is affiliated with two codes namely C_0 and C_1 for encoding "0" and "1," respectively, and also has two decoders for decoding "0" and "1." Since we have assumed that the random variable at the output of each decoder are statistically independent and have Gaussian distributions, their difference is also Gaussian with a mean value that is equal to the difference in means of C_0 and C_1 and a variance that is the sum of the two output variances. Fig. 7 shows a typical $U \times U$, 2CK SPE-OCDMA system with TPA receiver structure. In the following sections, we obtained the performance of 2CK scheme in various jamming environments.

1) Pulse-Jammer: Let $Y_{{\rm TPA}_{C_k|d_i}}: k = 0, 1$, denote the output random variable of decoder C_k. Without any loss of generality, we assume that the target user has transmitted bit "1"; therefore, at the output of decoder C_1 we can write N_s as

$$N_s = N_T + \frac{lmG}{N_0} + \frac{m_J G}{\rho N_0} \tag{60}$$

substituting (60) in (A.1)–(A.6), the mean and the variance of random variable $Y_{{\rm TPA}_{C_1|1}}$ can be evaluated such that $Y_{{\rm TPA}_{C_1|1}} \sim N(m_{C_1|1}, \sigma^2_{C_1|1})$. Also, at the output of decoder C_0, we can write N_s as

$$N_s = N_T + \frac{(l+1)mG}{N_0} + \frac{m_J G}{\rho N_0}. \tag{61}$$

Similar to the $Y_{{\rm TPA}_{C_1|1}}$, we can write $Y_{{\rm TPA}_{C_0|1}} \sim N(m_{C_0|1}, \sigma^2_{C_0|1})$. Then, the final random variable, i.e., $\Delta Y_{{\rm TPA}|1} = Y_{{\rm TPA}_{C_1|1}} - Y_{{\rm TPA}_{C_0|1}}$ can be written as

$$\Delta Y_{{\rm TPA}|1} \sim N\left(m_{C_1|1} - m_{C_0|1}, \sigma^2_{C_1|1} + \sigma^2_{C_0|1}\right). \tag{62}$$

So the error probability when bit "1" is transmitted can be evaluated as

$$P_{e|1} = P_r(\Delta Y_{{\rm TPA}|1} < 0) = Q\left(\frac{m_{C_1|1} - m_{C_0|1}}{\sqrt{\sigma^2_{C_1|1} + \sigma^2_{C_0|1}}}\right). \tag{63}$$

Because there is symmetry in the system, it is obvious that $P_{e|1} = P_{e|0}$; so $P_e = P_{e|1}$. Expectation over $P_{e|1}$ reduces the system error probability to (33).

2) Partial-Band Jammer: In this case, it is sufficient to update the mean and the variance of output random variable by computing N_s. If we assume that bit "1" is transmitted at the output of decoder C_1, we have $N_s = N_T + (lmG/N_0) + (m_J G/M_0)$ and at the output of decoder C_0 we have $N_s = N_T + ((l+1)mG/N_0) + (m_J G/M_0)$. Now similar to PJ, the error probability for PBJ can be written as

$$P_e = \sum_{l=0}^{U-1} Q\left(\frac{m_{C_1|1} - m_{C_0|1}}{\sqrt{\sigma^2_{C_1|1} + \sigma^2_{C_0|1}}}\right) \cdot p_{\rm 2CK}(l). \tag{64}$$

3) Follower-Jammer: Following the same trend, we assume that the transmitted signal of an FJ system is similar to (51). But we know that the user transmits bit "0" by encoding the pulse with code C_0 and bit "1" by encoding with code C_1. At the output of decoder C_0, the $\overline{m}$ and N_s can be evaluated as

$$\overline{m} = m(\overline{d_i}\sqrt{G} + \overline{d_J}\sqrt{L})^2 \tag{65}$$

$$N_s = N_T + \frac{m\left((d_i + l)G + (d_J + l_J)L\right)}{N_0}. \tag{66}$$

Substituting (65) and (66) in (A.1), the mean and the variance of the output Gaussian random variable of decoder C_0 denoted as $Y_{{\rm TPA}_{C_0|d_J,d_i}}$ can be evaluated, i.e., $Y_{{\rm TPA}_{C_0|d_J,d_i}} \sim N(m_{C_0|d_J,d_i}, \sigma^2_{C_0|d_J,d_i})$. And, for the output of decoder C_1, we can write

$$\overline{m} = m(d_i\sqrt{G} + d_J\sqrt{L})^2 \tag{67}$$

$$N_s = N_T + \frac{m\left((\overline{d_i} + l)G + (\overline{d_J} + l_J)L\right)}{N_0}. \tag{68}$$

Therefore by denoting the output random variable of decoder C_1 as $Y_{{\rm TPA}_{C_1|d_J,d_i}}$ then $Y_{{\rm TPA}_{C_1|d_J,d_i}} \sim N(m_{C_1|d_J,d_i}, \sigma^2_{C_1|d_J,d_i})$. The final output random variable can be written as

$$Y_{{\rm TPA}|d_J,d_i} = Y_{{\rm TPA}_{C_1|d_J,d_i}} - Y_{{\rm TPA}_{C_0|d_J,d_i}}, \quad d_J, d_i = 0, 1. \tag{69}$$

Since the output random variable of decoders C_0 and C_1 are independent, $Y_{{\rm TPA}|d_J,d_i}$ has also Gaussian distribution and can be expressed as

$$Y_{{\rm TPA}|d_J,d_i} \sim N\Big(m_{C_1|d_J,d_i} - m_{C_0|d_J,d_i}, \sigma^2_{C_1|d_J,d_i} + \sigma^2_{C_0|d_J,d_i}\Big). \tag{70}$$

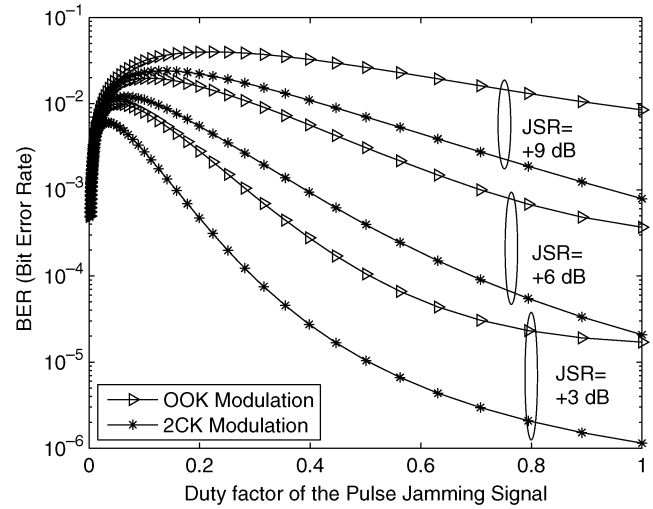

Fig. 8. BER versus duty factor of the PJ for $\mathrm{JSR} = 3, 6$, and 9 dB and OOK and $2\mathrm{CK}$ modulations.

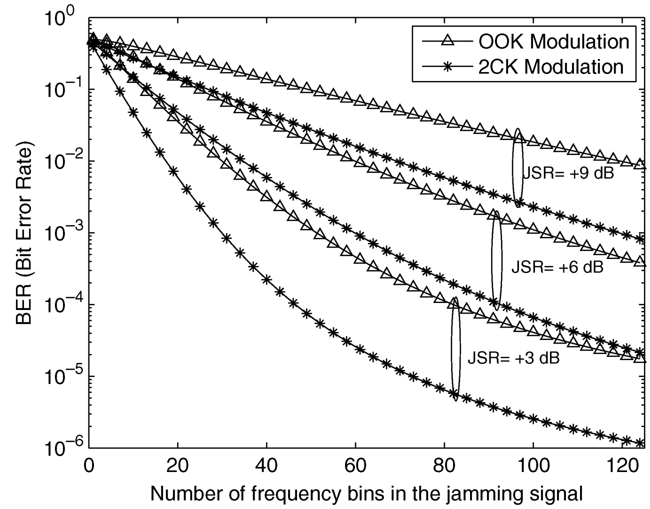

Fig. 9. BER versus number of frequency bins of the PBJ for $\mathrm{JSR} = 3, 6$, and 9 dB and OOK and $2\mathrm{CK}$ modulations.

Therefore, the conditional error probability can be written as

$$P_{e|l_J,l} = \frac{1}{4}\left\{P_r(Y_{\mathrm{TPA}|00} > 0) + P_r(Y_{\mathrm{TPA}|01} < 0) + P_r(Y_{\mathrm{TPA}|10} > 0) + P_r(Y_{\mathrm{TPA}|11} < 0)\right\}. \quad (71)$$

Since there is a symmetry in the system $P_{e|l_J,l}$ can be rewritten as

$$P_{e|l_J,l} = \frac{1}{2}P_r(Y_{\mathrm{TPA}|00} > 0) + P_r(Y_{\mathrm{TPA}|01} < 0). \quad (72)$$

Computing the mean and the variance of the two random variables, i.e., $Y_{\mathrm{TPA}|00}$ and $Y_{\mathrm{TPA}|01}$, the probabilities can be evaluated as

$$P_r(Y_{\mathrm{TPA}|00} > 0) = Q\left(-\frac{m_{C_1|00} - m_{C_0|00}}{\sqrt{\sigma^2_{C_1|00} + \sigma^2_{C_0|00}}}\right) \quad (73)$$

$$P_r(Y_{\mathrm{TPA}|01} < 0) = Q\left(\frac{m_{C_1|01} - m_{C_0|01}}{\sqrt{\sigma^2_{C_1|01} + \sigma^2_{C_0|01}}}\right). \quad (74)$$

Finally, the error probability can be computed as

$$P_e = \sum_{l=0}^{U-1}\sum_{l_J=0}^{U-1} P_{e|l_J,l} \cdot p_{2\mathrm{CK}}(l_J) \cdot p_{2\mathrm{CK}}(l). \quad (75)$$

V. Numerical Results

In this section, based on the performance analysis presented in Section III and IV, the numerical results for each system, i.e., ideal noiseless system with optimum detection and the suboptimum with nonlinear TPA system each with OOK and 2CK modulations, are discussed.

A. Ideal Noiseless System With Optimum Detection

For SPE-OCDMA system employing code length $N_0 = 128$, bit rate $R_b = 1$ Gbps, coherence time of the pulse $T_c = 400$ fs, and the number of users $U = 20$, the BER for both types of data modulation, i.e., OOK and $2\mathrm{CK}$, in the presence of different jammer scenarios are demonstrated in Figs. 8-10. Also, it is worth mentioning that the BER of the system without jamming signal is 2.5×10^{-7} and 3×10^{-8} for OOK and $2\mathrm{CK}$ modulations, respectively.

The BER of the system in the presence of a PJ for several values of JSR versus duty factor ρ is plotted in Fig. 8. As observed, the system performance in the presence of a PJ is substantially degraded. It can be seen that PJ has an optimized duty factor, namely, ρ_{opt} to maximize the BER. That is, if the jammer transmits its jamming pulses over a fraction of time, i.e., $\rho_{\mathrm{opt}} \approx 0.08$–$0.1$, then it is more effective than sending its pulses all the time with a constant average power J. As expected, as JSR increases, BER and ρ_{opt} increase as well. The resistance of the system using $2\mathrm{CK}$ as opposed to OOK modulation against PJ attack is quite evident; also one of the great advantage of using $2\mathrm{CK}$ modulation is zero threshold that is always optimum.

Fig. 9 shows the BER of the SPE-OCDMA system in a partial-band jamming environment versus the number of frequency bins of the spectrum of the jamming signal (M_0). It is observed, that for constant jammer power (J), as the bandwidth of the jamming signal increases, the BER decreases. This is due to the fact that the variance of the noise-like signal due to the jammer is $\sigma^2_{\mathrm{noise-like}} = J/M_0$; hence, the larger the M_0 the less effective the jammer. Hence, if the PBJ sends its pulses with a narrower spectrum, it can be more effective in degrading the system performance. As expected, the resistance of $2\mathrm{CK}$-system against PBJ is more than the OOK-system, by one order of magnitude.

Fig. 10 shows the BER of an SPE-OCDMA system in the presence of the FJ. The BER is plotted for several values of MAI users versus the jammer path loss. This jammer is the strongest jammer because the jamming signal is highly correlated with the desired signal and can effectively change the mean value of the received signals. So, if the jammer properly process and amplify the intercepted signal, it can severely degrade the performance of the system since the BER of the system without jamming signal for $U = 40$ is 4×10^{-6} and 10^{-6} for OOK and 2CK modulations, respectively. It can be seen that the BER of the

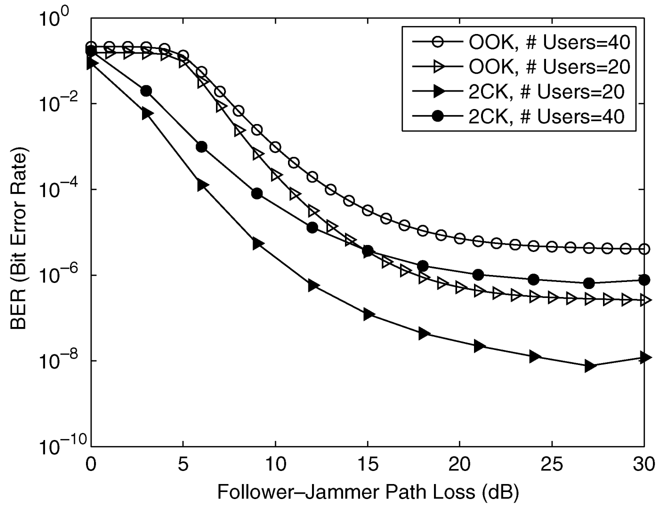

Fig. 10. BER versus FJ path loss for $U = 40$, 20 users and OOK and $2\mathrm{CK}$ modulations.

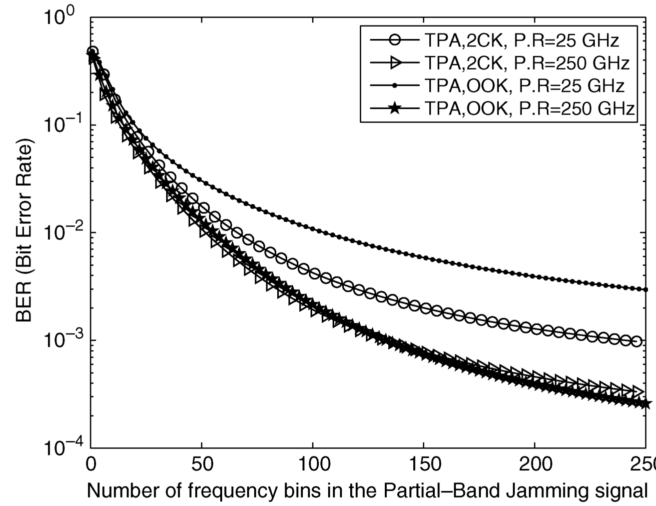

Fig. 12. BER versus number of frequency bins of PBJ for photodetector speed of 25, 250 GHz, and OOK and $2\mathrm{CK}$ modulations.

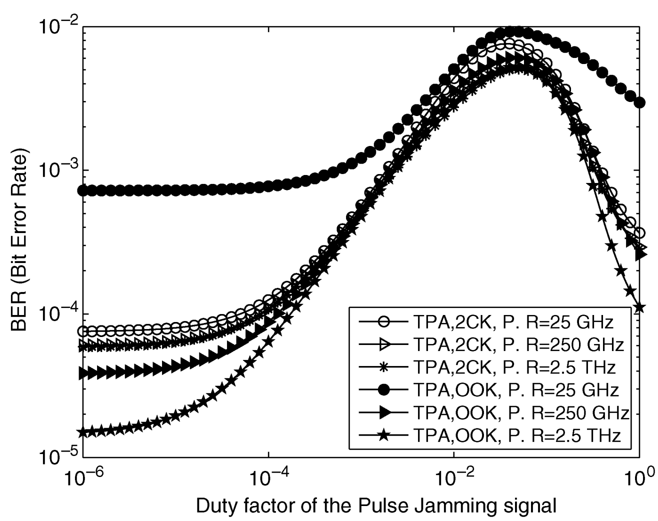

Fig. 11. BER versus duty factor of the PJ for photodetector speed of 25, 250 GHz, 2.5 THz, and OOK and $2\mathrm{CK}$ modulations.

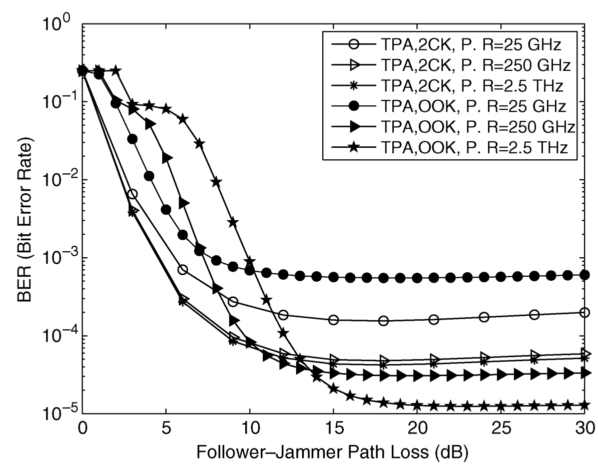

Fig. 13. BER versus FJ path loss for photodetector speed of 25, 250 GHz, 2.5 THz, and OOK and $2\mathrm{CK}$ modulations.

OOK system is almost constant when the FJ path loss is negligible; but, in a $2\mathrm{CK}$ system, the BER decreases as the FJ path loss increases; this is a direct result of zero threshold for $2\mathrm{CK}$ modulation. Therefore, we can conclude that the resistance of $2\mathrm{CK}$ system against various jammers is always more than the resistance of an OOK system.

B. Numerical Result of Nonlinear TPA Receiver

The BER of a system that uses TPA receiver for different cases is sketched in Figs. 11-13 using the parameters specified in Table I. As discussed before, most of the energy of the decoded pulse is assumed to be within a chip time [11]; this fact is used in analyzing the performance of TPA receiver Gaussian approximation. Also, it is worth mentioning that the BER of the system using OOK modulation without jamming signal is 2×10^{-5}, 4×10^{-5} and 7×10^{-4} for 2.5 THz, 250 GHz, and 25 GHz receiver, respectively, and the BER of the system using $2\mathrm{CK}$ modulation without jamming signal is 6×10^{-5}, 7×10^{-5}, and 3×10^{-4} for 2.5 THz, 250 GHz, and 25 GHz receiver, respectively.

The BER of a typical SPE-OCDMA system with TPA receiver and OOK and $2\mathrm{CK}$ modulation for various photodetector speeds in the presence of PJ is sketched in Fig. 11. It can be seen that for both types of modulation, the PJ degrade the system performance specially at its optimum duty factor ρ_{opt} at about 0.05. Also, it is obvious as the speed of the photodetector increases the system performance enhances as expected. As shown in this figure, when the PJ degrades the system performance at its ρ_{opt}, there is no noticeable difference between the performance of OOK and $2\mathrm{CK}$ systems.

Fig. 12 shows the BER of a system with TPA receiver for OOK and $2\mathrm{CK}$ modulation in the presence of a PBJ for 25 and 250 GHz receiver. As expected, the performance of the system degrades as the PBJ sends its pulses with a narrower frequency bandwidth. Fig. 12 shows that when the speed of photodetector is 25 GHz, the system with $2\mathrm{CK}$ modulation has a better performance than the OOK modulation against PBJ attack. But, when the speed increases both modulation schemes behave similarly.

Fig. 13 shows the BER of a system with a TPA receiver for OOK and $2\mathrm{CK}$ modulation in the presence of an FJ for 25,

TABLE I
TYPICAL VALUES USED IN THIS PAPER FOR TPA-RECEIVER

n_{sp}	Spontaneous Emission Factor	1.1
T_r	Receiver Temperature	300 K
R_L	Load Resistance	1000 Ω
T_c	Width of Ultrashort pulse	400 fsec
η	Photodetector quantum efficiency	0.8
k_3	Detection Efficiency in TPA receiver	5.0e-11 for T_c
N_0	Code length	250
U	Number of Users	10
R	Bit Rate	1 $Gbps$
G_{amp}	Gain of Amplifier	1000($3dB$)
L_1	Total path loss before amplification	8 dB
L_2	Total path loss after amplification	5 dB
m	Average number of transmitted photons by the users	10^6
m_J	Average number of transmitted photons by the jammer	10^6

250 GHz, and 2.5 THz receiver. It is demonstrated that, as the FJ path loss increases the system performance improves. This figure shows that in this attack the system using 2CK modulation can resist more against the FJ attack than the system using OOK modulation. Since the optimum threshold in 2CK modulation is always zero, the BER of such a system decreases faster when the FJ is strong, i.e., in low path loss conditions.

VI. DISCUSSION AND CONCLUSION

In this paper, we introduced, modeled, and analyzed three types of the jamming signals and their effects on the performance of two types of receiver structures of SPE-OCDMA systems, optimum and TPA receiver structures. In the former, thermal and quantum noises are neglected. In essence, the system performance degrades due to MAI and the jamming signals. It is shown that various jamming signals can degrade the performance of the system dramatically under certain conditions. We have also considered two types of modulation in each case, and it is shown that the system using 2CK rather than OOK modulation obtains a better performance against jamming signals. Since the speed of photodetector is less than the bandwidth of MLL's pulses, a nonlinear receiver, e.g., TPA receiver is suggested to improve the system performance. Therefore, in the latter system, the SPE-OCDMA system using TPA receiver is considered. The performance with TPA includes various noises such as thermal noise, optical amplifier's noise, and shot noise along with MAI and the jamming signals. It is shown that jamming signals can severely degrade the performance of such systems also. In TPA receiver, the performances of OOK and 2CK systems are similar, but the performance of 2CK system in the presence of the FJ is better than the OOK system. Furthermore in OOK systems, we assume that the receiver obtains the optimal threshold, which is obtained by a great deal of effort, but in 2CK modulation the optimal threshold is zero and there is no computational complexity. For both systems, we show that as the code length (N_0) increases, the performance of the system improves when facing PJ; however, this solution is not effective against partial-band and FJ attacks. If the receiver randomly processes some frequency bins of the pulse spectrum, it is expected that the effect of the partial-band jamming signals reduces too. For FJ, randomly changing users' codes with a speed faster than the processing rate of the FJ can be effective in such jamming environments.

APPENDIX A

In this Appendix, we obtain the mean and the variance of received signal using the method described in [15]. The mean and the variance of the random variable, Y_{TPA}, can be evaluated as

$$E\{Y_{\mathrm{TPA}}\} = \eta k_3\left(\overline{m}^2 + 4\overline{m}N_s + 2MN_s^2\right) \quad \text{(A.1)}$$

$$\begin{aligned} E\left\{Y_{\mathrm{TPA}}^2\right\} = \eta^2 k_3^2\big(&\overline{m}^4 + 16\overline{m}^3 Ns + 68\overline{m}^2 Ns^2 + 48\overline{m}Ns^3 \\ &+ 16\overline{m}Ns^3(M+2) + 4M\overline{m}^2 Ns^2 \\ &+(4M^2 + 20M)Ns^4\big) \end{aligned} \quad \text{(A.2)}$$

where η is the quantum efficiency, k_3 is defined in [15] as $k_3 \triangleq (12Vhf/16S^2T)$ (V is the volume of photodetector, T is the integration time of photodetector, and S is the area of TPA photodetector), $\overline{m}$ is the average number of received photons, N_s is the power spectral density of the noise, and M is the number of modes in the received signal which depends on the speed of the receiver photodetector [15]. These parameters can be evaluated as

$$G = G_{\mathrm{amp}} L_1 L_2 / U \quad \text{(A.3)}$$

$$\overline{m} \triangleq mG \quad \text{(A.4)}$$

$$N_T = n_{\mathrm{sp}}(G_{\mathrm{amp}} - 1)L_2 \quad \text{(A.5)}$$

$$N_S = N_T + l\frac{mG}{N_0} \quad \text{(A.6)}$$

where G_{amp} is the optical amplifier gain, L_1 and L_2 are the losses before and after the star coupler, U is the number of network's users, N_T is the power spectral density of the amplifier noise, n_{sp} is the spontaneous emission factor of the optical amplifier, N_s is due to the amplifier noise and the presence of other users' signal as improperly decoded interference signal. It is assumed that the bandwidth of the filter is equal to the bandwidth of the signal, i.e., B_0. Without any loss of generality and for the sake of mathematical simplicity, it is assumed that $M = B_0 T = 2L+1$, which is the total number of longitudinal modes or samples in the received signal [15].

In our performance analysis, we include the shot noise and thermal noise effects. So the mean and variance of the random variable, Y_{TPA}, can be evaluated as

$$\mathrm{Var}(Y_{\mathrm{TPA}}) = E\{Y_{\mathrm{TPA}}\} + \left(E\left\{Y_{\mathrm{TPA}}^2\right\} - E^2\{Y_{\mathrm{TPA}}\}\right) + \sigma_{\mathrm{Th}}^2 \quad \text{(A.7)}$$

where $\sigma_{\mathrm{Th}}^2 = 2k_B T_r T/q^2 R_L$ is the variance of the thermal noise. In this expression, k_B is the Boltzmann's constant, T_r is the equivalent temperature of the receiver, T is the integration time period, q is the electron charge, and R_L is the resistance of load, which is seen from the photodetector input.

REFERENCES

[1] J. A. Salehi, A. M. Weiner, and J. P. Heritage, "Coherent ultrashort light pulse code-division multiple access communication systems," *J. Lightw. Technol.*, vol. 8, no. 3, pp. 478–491, Mar. 1990.

[2] S. Etemad, P. Toliver, R. Menendez, J. Young, T. Banwell, S. Galli, J. Jackel, P. Delfyett, C. Price, and T. Turpin, "Spectrally efficient optical CDMA using coherent phase-frequency coding," *IEEE Photon. Technol. Lett.*, vol. 17, no. 4, pp. 929–931, Apr. 2005.

[3] R. P. Scott, W. Cong, K. Li, V. J. Hernandez, B. H. Kolner, J. P. Heritage, and S. J. B. Yoo, "Demonstration of an errorfree 4/spl times/10 Gb/s multiuser SPECTS O-CDMA network testbed," *IEEE Photon. Technol. Lett.*, vol. 16, no. 9, pp. 2186–2188, Sep. 2004.

[4] R. A. Poisol, *Modern Communications Jamming Principles and Techniques*. Norwood, MA: Artech House, 2004.

[5] T. Shake, "Security performance of optical CDMA against eavesdropping," *J. Lightw. Technol.*, vol. 23, no. 2, pp. 655–670, Feb. 2005.

[6] T. Shake, "Confidentiality performance spectral-phase-encoded optical CDMA," *J. Lightw. Technol.*, vol. 23, no. 4, pp. 1652–1663, Apr. 2005.

[7] Z. Jiang, D. Learid, and A. M. Weiner, "Experimental investigation of security issues in O-CDMA," *J. Lightw. Technol.*, vol. 24, no. 11, pp. 4228–4234, Nov. 2006.

[8] A. M. Weiner, Z. Jiang, and D. Learid, "Spectrally phase encoded OCDMA [invited]," *J. Opt. Netw.*, vol. 6, no. 6, pp. 728–755, 2007.

[9] X. Wang, N. Wada, T. Miyazaki, and K. Kitayama, "Coherent OCDMA system using DPSK data format with balanced detection," *IEEE Photon. Technol. Lett.*, vol. 18, no. 7, pp. 826–828, Apr. 2006.

[10] J. A. Salehi, "Emerging optical CDMA communication systems and data networks [invited]," *J. Opt. Netw.*, vol. 6, no. 9, pp. 1138–1178, 2007.

[11] K. Jamshidi and J. A. Salehi, "Performance analysis of spectral-phase-encoded optical CDMA system using two-photon-absorption receiver structure for asynchronous and slot-level synchronous transmitters," *J. Lightw. Technol.*, vol. 25, no. 6, pp. 1638–1645, Jun. 2007.

[12] K. Jamshidi and J. A. Salehi, "Statistical analysis of coherent ultrashort light pulse CDMA with multiple optical amplifiers using additive noise model," *J. Lightw. Technol.*, vol. 23, no. 5, pp. 1842–1851, May 2005.

[13] M. Rochette and A. Rusch, "Spectral efficiency of OCDMA systems with coherent pulse sources," *J. Lightw. Technol.*, vol. 23, no. 3, pp. 1033–1038, Mar. 2005.

[14] M. K. Simon, J. K. Omura, R. A. Scholtz, and B. K. Levitt, *Spread Spectrum Communications*. Rockville, MD: Computer Science, 1985.

[15] K. Jamshidi and J. A. Salehi, "Statistical characterization and bit-error rate analysis of lightwave systems with optical amplification using two-photon-absorption receiver structures," *J. Lightw. Technol.*, vol. 24, no. 3, pp. 1302–1316, Mar. 2006.

[16] Z. Zheng, A. M. Weiner, J. H. Marsh, and M. M. Karkhanechi, "Ultrafast optical thresholding based on two-photon absorption GaAs waveguide photodetectors," *IEEE Photon. Technol., Lett.*, vol. 9, no. 4, pp. 493–495, Apr. 1997.

[17] Z. Zheng, H. Sardesai, C. C. Chang, S. Shen, A. M. Weiner, J. H. Marsh, and M. M. Karkhanechi, "Nonlinear detection of spectrally coded ultrashort pulse by two-photon absorption GaAs photodetectors," in *Proc. Conf. Lasers Electro-Opt. (CLEO)*, San Francisco, CA, 1998, pp. 97–98.

Mohammad J. Emadi was born in Shiraz, Iran, on November 13, 1983. He received the B.S. degree from Amirkabir University of Technology (AUT) (with honors), Tehran, Iran, in 2006, and the M.S. degree in electrical engineering from Sharif University of Technology (SUT), Tehran, in 2008, where currently he is working toward the Ph.D. degree in the Department of Electrical Engineering.

Since 2006, he has been with Optical Networks Research Lab (ONRL) as a member of technical staff. His research interests include wireless optical and fiber-optic communication systems, optical CDMA, and multiple-access communications.

Jawad A. Salehi (M'84–SM'07) was born in Kazemain, Iraq, on December 22, 1956. He received the B.S. degree from the University of California, Irvine, in 1979, and the M.S. and Ph.D. degrees from the University of Southern California (USC), Los Angeles, in 1980 and 1984, respectively, all in electrical engineering.

From 1981 to 1984, he was a Full-Time Research Assistant at the Communication Science Institute, USC. From 1984 to 1993, he was a Member of Technical Staff of the Applied Research Area, Bell Communications Research (Bellcore). During 1990, he was with the Laboratory of Information and Decision Systems, Massachusetts Institute of Technology (MIT), Cambridge, as a Visiting Research Scientist. From 1999 to 2001, he was the Head of the Mobile Communications Systems Group and the Co-Director of the Advanced and Wideband Code-Division Multiple Access (CDMA) Laboratory, Iran Telecom Research Center (ITRC). From 2003 to 2006, he was the Director of the National Center of Excellence in Communications Science, Department of Electrical Engineering, SUT. Currently, he is a Full Professor at the Optical Networks Research Laboratory (ONRL), Department of Electrical Engineering, Sharif University of Technology (SUT), Tehran, Iran, where he is also the Co-Founder of the Advanced Communications Research Institute (ACRI). He is the holder of 12 US patents on optical CDMA. His current research interests include optical multiaccess networks, optical orthogonal codes (OOC), fiber-optic CDMA, femtosecond or ultrashort light pulse CDMA, spread-time CDMA, holographic CDMA, wireless indoor optical CDMA, all-optical synchronization, and applications of erbium-doped fiber amplifiers in optical systems.

Dr. Salehi is an Associate Editor for Optical CDMA of the IEEE TRANSACTIONS ON COMMUNICATIONS since May 2001. In September 2005, he was elected as the Interim Chair of the IEEE Iran Section. He was the recipient of several awards including the Bellcore's Award of Excellence, the Nationwide Outstanding Research Award from the Ministry of Science, Research, and Technology in 2003, and the Nation's Highly Cited Researcher Award in 2004. In 2007, he received Khwarazmi International prize, first rank, in fundamental research and also the outstanding Inventor Award (Gold medal) from World Intellectual Property Organization (WIPO), Geneva, Switzerland. He is among the 250 preeminent and most influential researchers worldwide in the *Institute for Scientific Information (ISI) Highly Cited* in the Computer-Science Category. He is the corecipient of the IEEE's Best Paper Award in 2004 from the International Symposium on Communications and Information Technology, Sapporo, Japan.